# Time-Domain Full Waveform Inversion for High Resolution 3D Ultrasound Computed Tomography of the Breast

Felix Lucka

**International Workshop on Medical Ultrasound Tomography**
Detroit
15the October 2019

# H2020 Project: Novel PAT+USCT Mammography Scanner

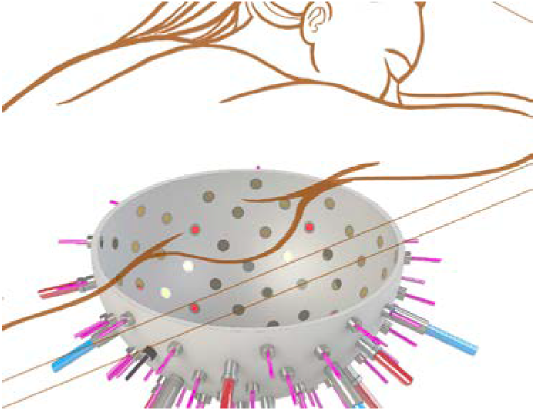

**Diagnostic information from optical and acoustic properties**

- 512 US transducers on rotatable half-sphere
- 40 optical fibers for photoacoustic excitation
- 40 inserts for laser-induced US (LIUS)

# H2020 Project: Partners

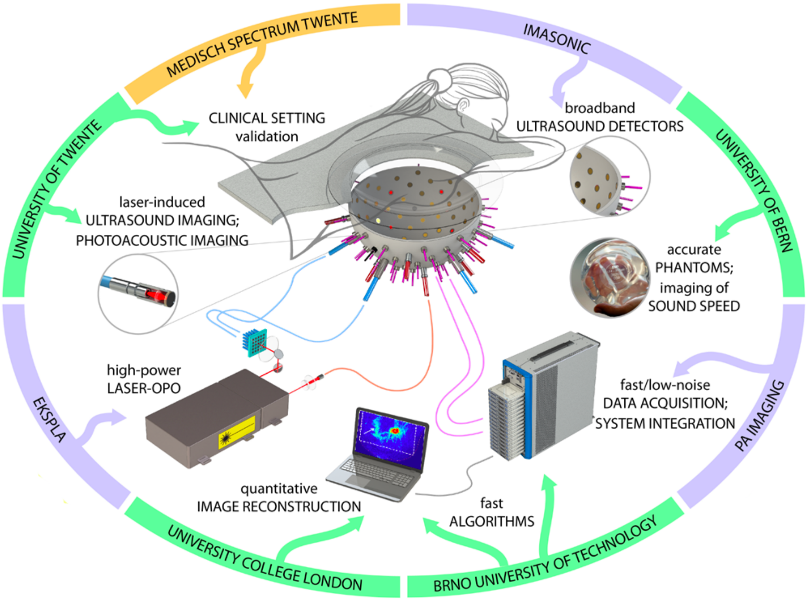

# USCT Reconstruction Approaches

$$(c(x)^{-2}\partial_t^2 - \Delta)p_i(x,t) = s_i(x,t), \qquad f_i = M_i p_i, \qquad i = 1, \dots, n_{src}$$

**Travel time tomography (TTT)**: geometrical optics approximation.

✓ robust & computationally efficient

! valid for high frequencies ($\rightarrow$ attenuation), low res, data size

**Reverse time migration (RTM)**: forward wavefield correlated in time with backward wavefield (adjoint wave equation) via imaging condition.

✓ 2 wave simulations, better quality than TTT.

! approximation, needs initial guess, quantitative errors

**Full waveform inversion (FWI)**: fit full model to all data.

✓ high res from little data, include constraints, regularization

! many wave simulations, non-convex PDE-constrained optimization.

**time domain vs frequency domain methods**

# Time Domain Full Waveform Inversion

$$F(c)p_i := (c^{-2}\partial_t^2 - \Delta)p_i = s_i, \qquad f_i = M_i\, p_i, \quad i = 1, \dots, n_{src}$$

$$\min_{c \in \mathcal{C}} \sum_i^{n_{src}} \mathcal{D}\left(f_i(c), f_i^\delta\right) \quad s.t. \quad f_i(c) = M_i F^{-1}(c) s_i$$

gradient for **first-order optimization** via **adjoint state method**:

$$\nabla_c \mathcal{D}\left(f(c), f^\delta\right) = 2 \int_0^T \frac{1}{c(x)^3} \left(\frac{\partial^2 p(x,t)}{\partial t^2}\right) q^*(x,t) \quad ,$$

where $(c^{-2}\partial_t^2 - \Delta)q^* = s^*$, $s^*(x,t)$ is time-reversed data discrepancy

$\rightarrow$ **two wave simulations for one gradient**

# Acoustic Wave Propagation: Numerical Solution

- **Direct methods**, such as finite-difference, pseudospectral, finite/spectral element, discontinous Galerkin.
- **Integral wave equation methods**, e.g. boundary element
- **Asymptotic methods**, e.g., geometrical optics, Gaussian beams

## Acoustic Wave Propagation: Numerical Solution

- Direct methods, such as finite-difference, **pseudospectral**, finite/spectral element, discontinous Galerkin.
- Integral wave equation methods, e.g. boundary element.
- Asymptotic methods, e.g., geometrical optics, Gaussian beams.

**k-Wave**: *k*-space pseudospectral method solving the underlying system of first order conservation laws.

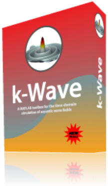


- Compute spatial derivatives in Fourier space: 3D FFTs.
- Parallel/GPU computing leads to massive speed-ups.
- Modify finite temporal differences by *k*-space operator and use staggered grids for accuracy and robustness.
- Perfectly matched layer to simulate free-space propagation.

**B. Treeby and B. Cox, 2010.** k-Wave: MATLAB toolbox for the simulation and reconstruction of photoacoustic wave fields, *Journal of Biomedical Optics.*

# Numerical Phantoms

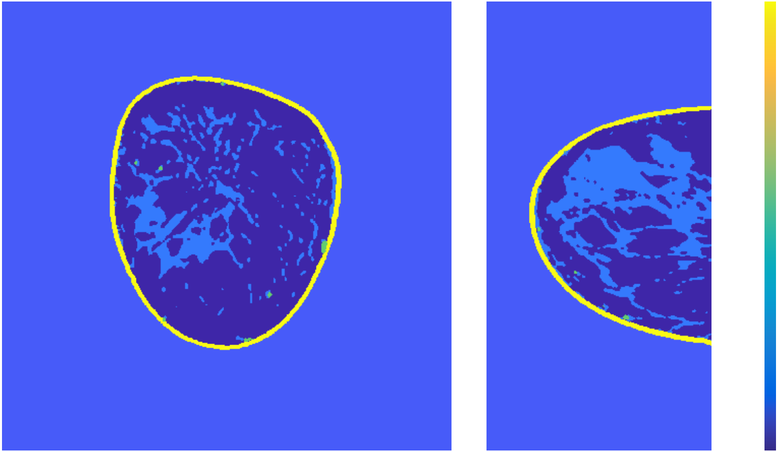

color range 1470 - 1650 m/s, resolution 0.5mm

**Yang Lou et al.** Generation of anatomically realistic numerical phantoms for photoacoustic and ultrasonic breast imaging, *JBO, 2017.*

https://anastasio.wustl.edu/downloadable-contents/oa-breast/

# Numerical Phantoms

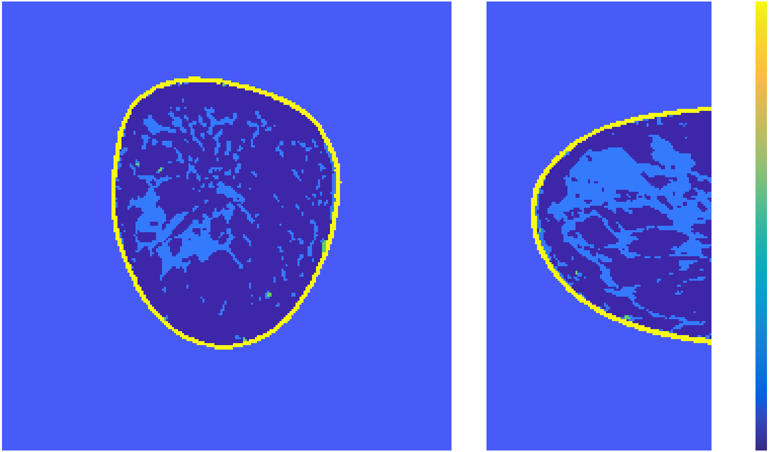

color range 1470 - 1650 m/s, resolution 1mm

**Yang Lou et al.** Generation of anatomically realistic numerical phantoms for photoacoustic and ultrasonic breast imaging, *JBO, 2017.*
https://anastasio.wustl.edu/downloadable-contents/oa-breast/

# FWI Illustration in 2D

SOS ground truth $c^{true}$

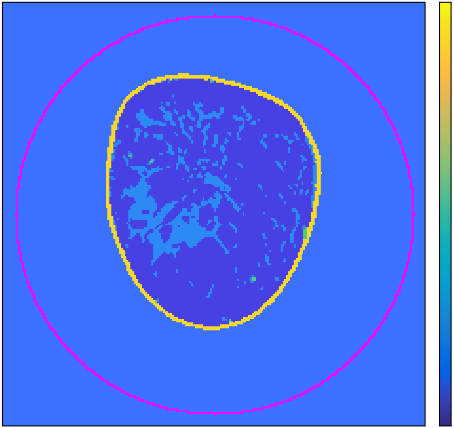

color range 1450 - 1670 m/s

- 1mm resolution
- $222^2$ voxel
- 836 voxels on surface (pink)
- TTT would need $836^2$ source-receiver combos for high res result

# FWI Illustration in 2D: 64 Sensors, 64 Receivers

SOS reconstruction $c^{rec}$

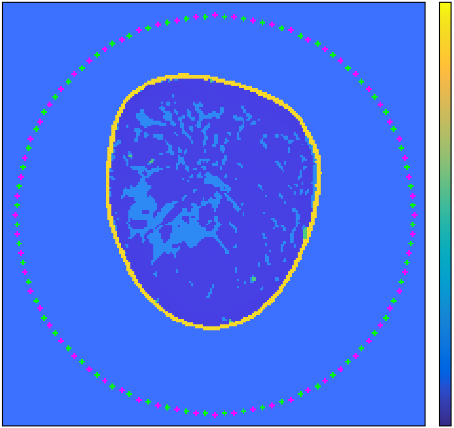

color range 1450 - 1670 m/s

reconstruction error $c^{true} - c^{rec}$

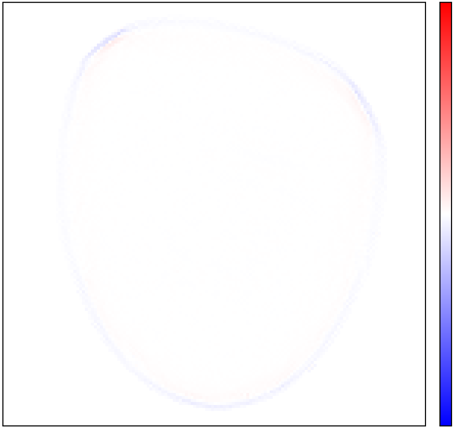

color range -50 - 50 m/s

# FWI Illustration in 2D: 32 Sensors, 32 Receivers

SOS reconstruction $c^{rec}$

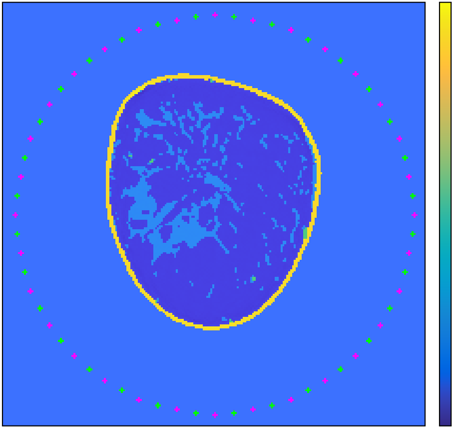

color range 1450 - 1670 m/s

reconstruction error $c^{true} - c^{rec}$

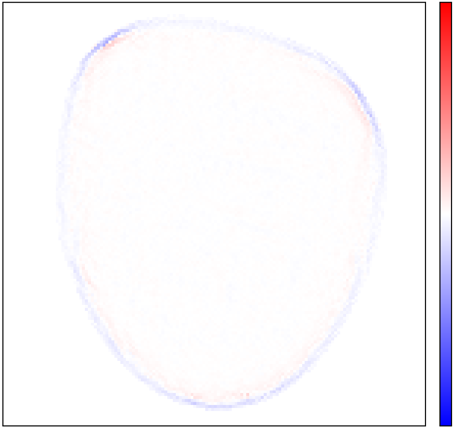

color range -50 - 50 m/s

# FWI Illustration in 2D: 16 Sensors, 16 Receivers

SOS reconstruction $c^{rec}$

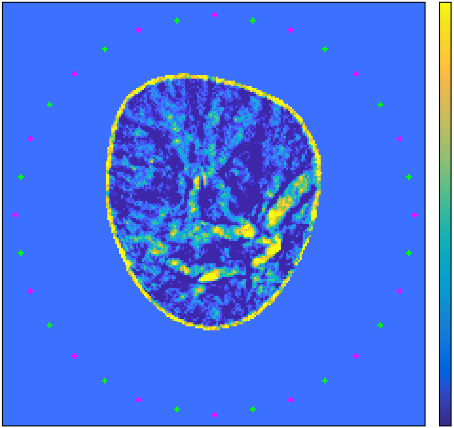

color range 1450 - 1670 m/s

reconstruction error $c^{true} - c^{rec}$

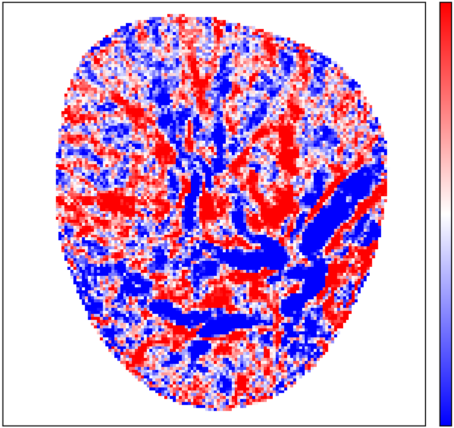

color range -50 - 50 m/s

# Challenges of High-Resolution FWI in 3D

$$\min_{c \in \mathcal{C}} \sum_{i}^{n_{src}} \mathcal{D}\left(f_i(c), f_i^\delta\right) \quad s.t. \quad f_i(c) = M_i F^{-1}(c) s_i$$

$$\nabla_c \mathcal{D}\left(f(c), f^\delta\right) = 2 \int_0^T \frac{1}{c(x)^3} \left(\frac{\partial^2 p(x,t)}{\partial t^2}\right) q^*(x,t)$$

PAMMOTH scanner example:

- 0.5mm res: comp grid $560 \times 560 \times 300$ voxel $= 94$M, ROI $= 7$M
- 1024 transducers, 4000 time samples (multiple sources);

Gradient computation:

- 1 wave sim: $\sim$30 min.

**!** **2 wave sim per source**, $n_{src} = 1024 \rightarrow 20$ days per gradient.

**!** **storage of forward field** in ROI: $\sim$ 200GB.

# Challenges of High-Resolution FWI in 3D

$$\min_{c \in \mathcal{C}} \sum_{i}^{n_{src}} \mathcal{D}\left(f_i(c), f_i^\delta\right) \quad s.t. \quad f_i(c) = M_i F^{-1}(c) s_i$$

$$\nabla_c \mathcal{D}\left(f(c), f^\delta\right) = 2 \int_0^T \frac{1}{c(x)^3} \left(\frac{\partial^2 p(x,t)}{\partial t^2}\right) q^*(x,t)$$

PAMMOTH scanner example:

- 0.5mm res: comp grid $560 \times 560 \times 300$ voxel $= 94$M, ROI $= 7$M
- 1024 transducers, 4000 time samples (multiple sources);

Gradient computation:

- 1 wave sim: $\sim$30 min.
- ! **2 wave sim per source**, $n_{src} = 1024 \rightarrow 20$ days per gradient.
  stochastic gradient methods $\rightarrow$ 60 min per gradient
- ! **storage of forward field** in ROI: $\sim$ 200GB.
  time-reversal based gradient computation $\rightarrow 5 - 25$GB.

# Stochastic Gradient Optimization

$$\mathcal{J} := n_{src}^{-1} \sum_{i}^{n_{src}} \mathcal{D}_i(c) := n_{src}^{-1} \sum_{i}^{n_{src}} \mathcal{D}\left(M_i F^{-1}(c) s_i, f_i^{\delta}\right)$$

approx $\nabla \mathcal{J}$ by $|\mathcal{S}|^{-1} \sum_{j \in \mathcal{S}} \nabla \mathcal{D}_j(c)$, $\mathcal{S} \subset \{1, \ldots, n_{src}\}$ predetermined.
$\rightarrow$ **incremental gradient, ordered sub-set methods**

# Stochastic Gradient Optimization

$$\mathcal{J} := n_{src}^{-1} \sum_{i}^{n_{src}} \mathcal{D}_i(c) := n_{src}^{-1} \sum_{i}^{n_{src}} \mathcal{D}\left(M_i F^{-1}(c) s_i, f_i^{\delta}\right)$$

approx $\nabla \mathcal{J}$ by $|\mathcal{S}|^{-1} \sum_{j \in \mathcal{S}} \nabla \mathcal{D}_j(c)$, $\mathcal{S} \subset \{1, \ldots, n_{src}\}$ predetermined.
$\rightarrow$ **incremental gradient, ordered sub-set methods**

Instance of **finite sum minimization** similar to **training in machine learning**. Use **stochastic gradient descent (SGD)**:

- momentum, gradient/iterate averaging (SAV, SAGA), variance reduction (SVRG), choice of step size, mini-batch size
- include non-smooth regularizers (SPDHG, SADMM)
- quasi-Newton-type methods, e.g., **stochastic L-BFGS**


**Bottou, Curtis, Nocedal.** Optimization Methods for Large-Scale Machine Learning, *arXiv:1606.04838.*

**Fabien-Ouellet, Gloaguen, Giroux, 2017.** A stochastic L-BFGS approach for full-waveform inversion, *SEG.*

## Gradient Estimates: Sub-Sampling vs Source Encoding

**Computationally & stochastically efficient** gradient estimator?

# Gradient Estimates: Sub-Sampling vs Source Encoding

**Computationally & stochastically efficient** gradient estimator?

**Source Encoding** for linear PDE constraints:

$$\text{Let} \quad \hat{s} := \sum_{i}^{n_{srt}} w_i s_i, \quad \hat{f}^{\delta} := \sum_{i}^{n_{srt}} w_i f_i^{\delta}, \quad \text{with} \quad \mathbb{E}\left[w\right] = 0, \ \mathbb{C}\text{ov}[w] = I,$$

$$\text{then} \quad \mathbb{E}\left[\nabla \left\| MF^{-1}(c)\hat{s} - \hat{f}^{\delta} \right\|_2^2\right] = \nabla \sum_{i}^{n_{src}} \left\| MF^{-1}(c)s_i - f_i^{\delta} \right\|_2^2$$

- related to covariance trace estimators
- Rademacher distribution ($w_i = \pm 1$ with equal prob)
- add time-shifting for time-invariant PDEs $\rightarrow$ variance control
- can be turned into scanning strategy

**Haber, Chung, Herrmann, 2012.** An effective method for parameter estimation with PDE constraints with multiple right-hand sides, *SIAM J. Optim.*

# Stochastic Optimization Illustration

SOS reconstruction $c^{rec}$ L-BFGS

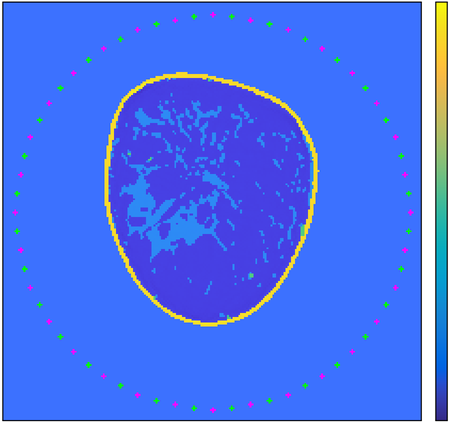

color range 1450 to 1670 m/s

reconstruction error $c^{true} - c^{rec}$

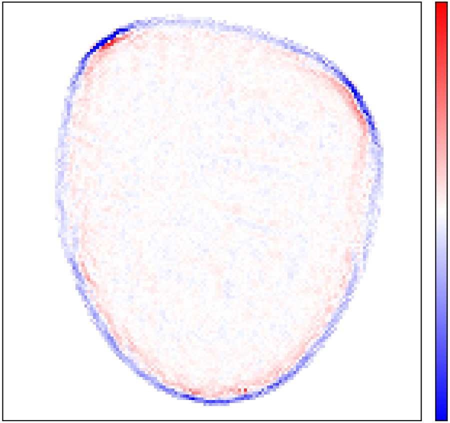

color range -10 to 10 m/s

# Stochastic Optimization Illustration

SOS reconstruction $c^{rec}$ SL-BFGS

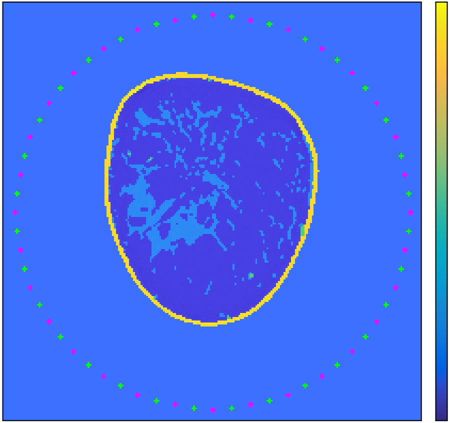

color range 1450 to 1670 m/s

reconstruction error $c^{true} - c^{rec}$

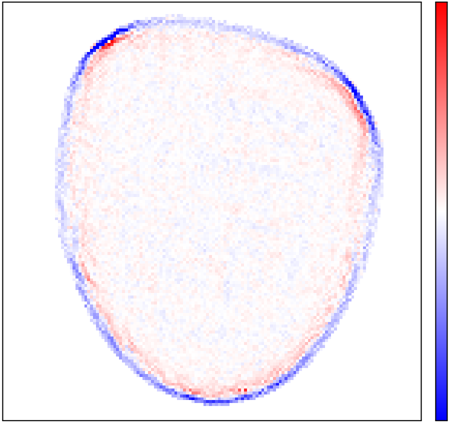

color range -10 to 10 m/s

# Time-Reversal Gradient Computations

**Avoid storage of forward fields!**

$$(c(x)^{-2}\partial_t^2 - \Delta)p(x,t) = s(x,t), \qquad \textit{in } \mathbb{R}^d \times [0,T]$$

$$\nabla_c \mathcal{D} = 2\int_0^T \frac{1}{c(x)^3}\left(\frac{\partial^2 p(x,t)}{\partial t^2}\right) q^*(x,t)$$

**Idea:** ROI $\Omega$, $\mathrm{supp}(s) \in \Omega^c \times [0,T]$. As $p(x,0) = p(x,T) = \partial_t p(x,0) = \partial_t p(x,T) = 0$ in $\Omega$, $p(x,t)$ can be reconstructed from $p(x,t)$ on $\partial\Omega \times [0,T]$ by **time-reversal (TR)**.

- store fwd fields on ROI boundary during forward wave simulation
- interleave backward (adjoint) simulation with TR of boundary data
- 3 instead of 2 wave simulations (unless 2 GPUs used).
- code up efficiently
- multi-layer boundary increases accuarcy for pseudospectral method

# Multigrid Schemes

- easy due to regular grids in space and time
- coarsening by 2: (in principle) **speed up of 16**
- most basic multi-grid usage for now: initialization

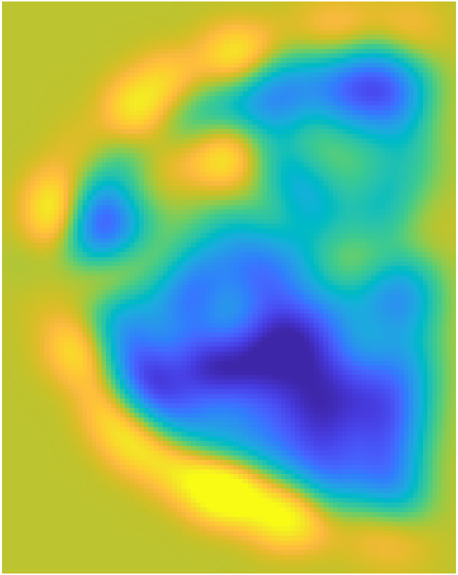

level 6: upsampled from 5.66mm.

# Multigrid Schemes

- easy due to regular grids in space and time
- coarsening by 2: (in principle) **speed up of 16**
- most basic multi-grid usage for now: initialization

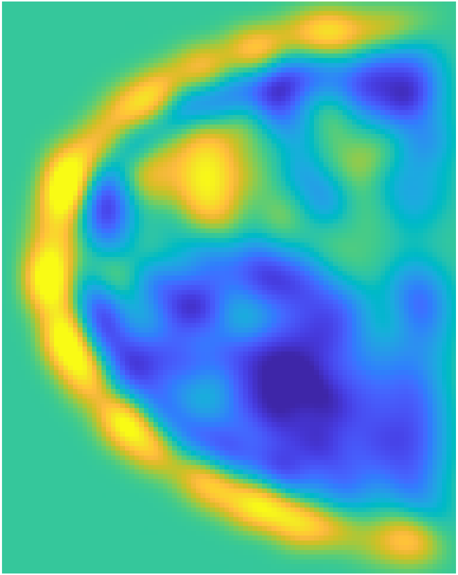

level 5: upsampled from 4mm.

# Multigrid Schemes

- easy due to regular grids in space and time
- coarsening by 2: (in principle) **speed up of 16**
- most basic multi-grid usage for now: initialization

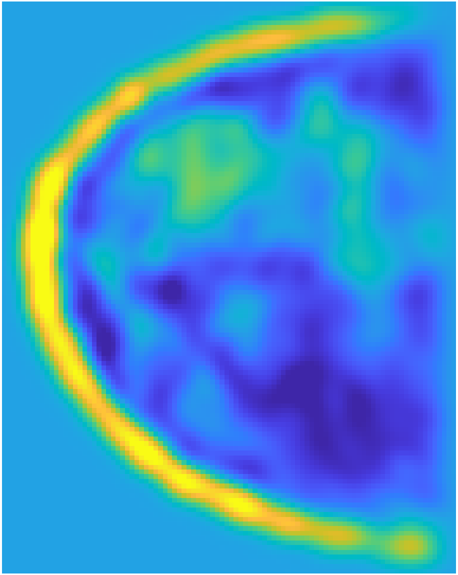

level 4: upsampled from 2.83mm.

# Multigrid Schemes

- easy due to regular grids in space and time
- coarsening by 2: (in principle) **speed up of 16**
- most basic multi-grid usage for now: initialization

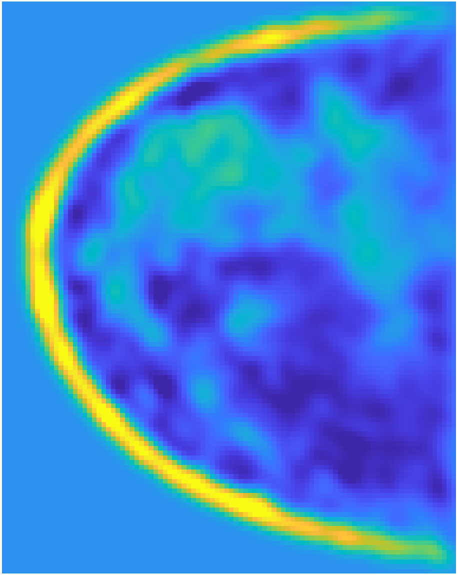

level 3: upsampled from 2mm.

# Multigrid Schemes

- easy due to regular grids in space and time
- coarsening by 2: (in principle) **speed up of 16**
- most basic multi-grid usage for now: initialization

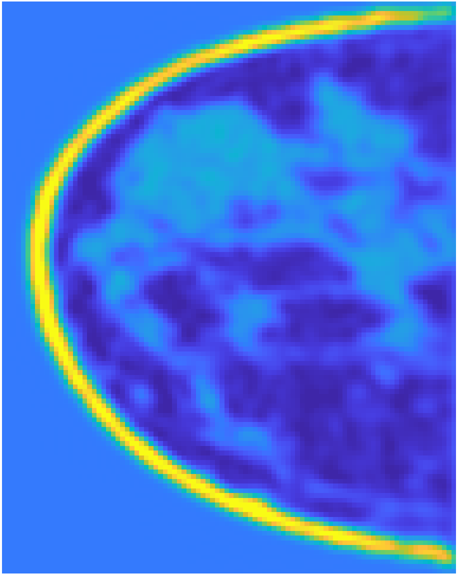

level 2: upsampled from 1.41mm.

# Multigrid Schemes

- easy due to regular grids in space and time
- coarsening by 2: (in principle) **speed up of 16**
- most basic multi-grid usage for now: initialization

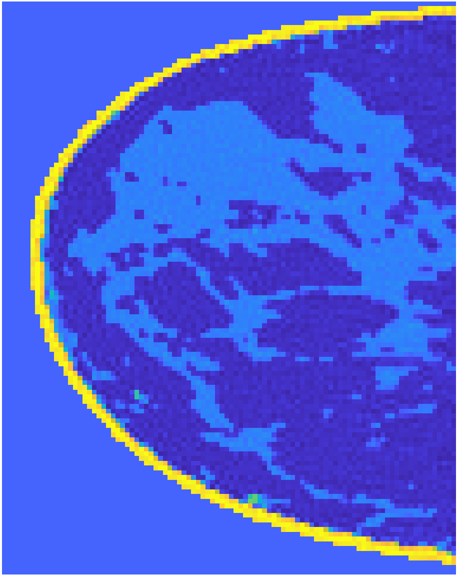

level 1: resolution 1mm

# Utilizing Multiple GPUs

- average independent gradient estimates to reduce variance
- not be the best way to use multiple GPUs

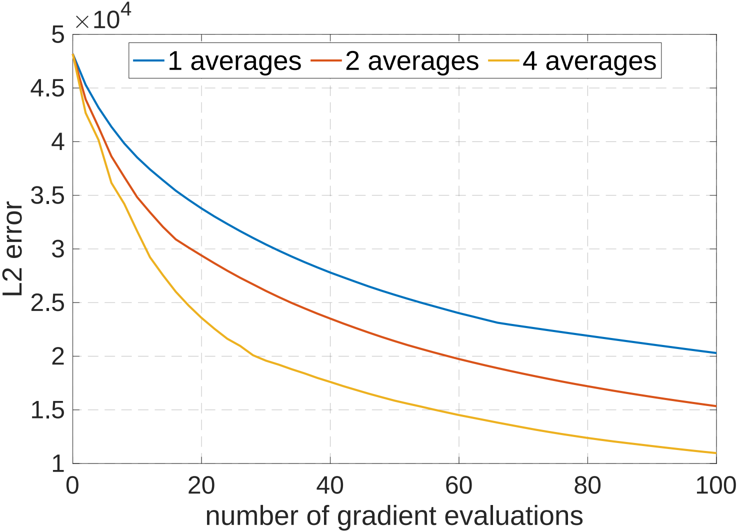

# Putting it all together

- 3D breast phantom at 0.5mm resolution, 1024 sources and receivers
- $442 \times 442 \times 232$ voxel, 3912 time steps
- multi-grid with 8 levels, coarsening factor $\sqrt{2}$.
- SL-BFGS (40 iter, 2d 4h on highest level), source encoding, 2 GPUs

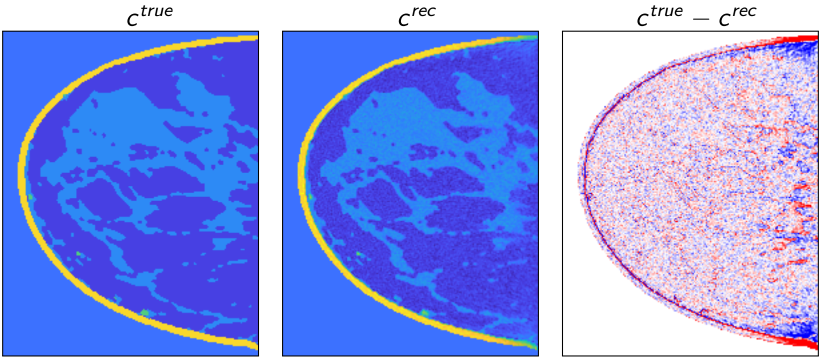


color range 1450 to 1670 m/s        color range -50 to 50 m/s

# Summary & Outlook

**Summary:**

- proof-of-concept studies of TD-FWI for high resolution 3D USCT
- stochastic L-BFGS with source encoding
- time reversal based gradient computation
- multi-grid initialization

**Outlook:**

- multi-GPU CUDA code
- realistic source/receiver modeling
- extension to acoustic attenuation, density, etc.
- **validation on experimental data!**

**L, Pérez-Liva, Treeby, Cox, 2019.** Time-Domain Full Waveform Inversion for High Resolution 3D Ultrasound Computed Tomography of the Breast, *in preparation.*

PHOTONICS PUBLIC PRIVATE PARTNERSHIP

PHOTONICS21

EPSRC

Engineering and Physical Sciences Research Council

NWO

NVIDIA

## Thank you for your attention!

**L, Pérez-Liva, Treeby, Cox, 2019.** Time-Domain Full Waveform Inversion for High Resolution 3D Ultrasound Computed Tomography of the Breast, *in preparation.*

PHOTONICS PUBLIC PRIVATE PARTNERSHIP

PHOTONICS21

EPSRC Engineering and Physical Sciences Research Council

NWO

NVIDIA

# Influence of Noise

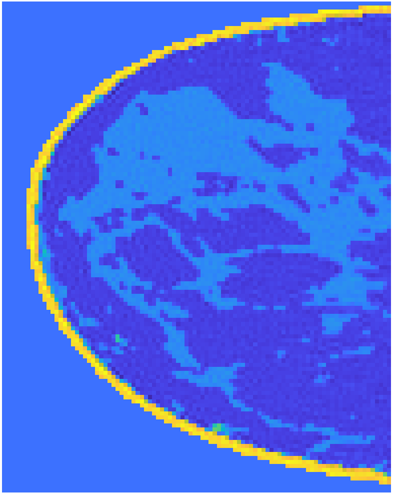

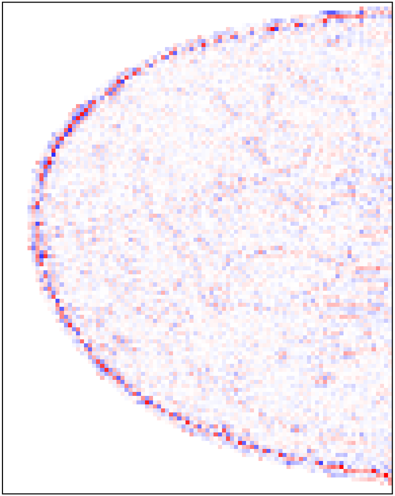

no noise

# Influence of Noise

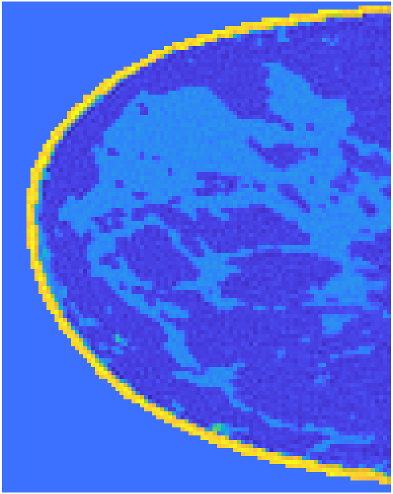

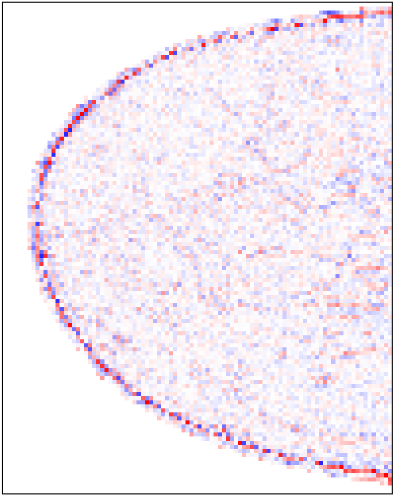

SNR 30dB

# Influence of Noise

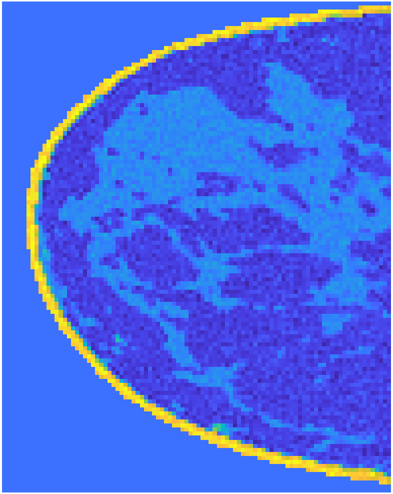

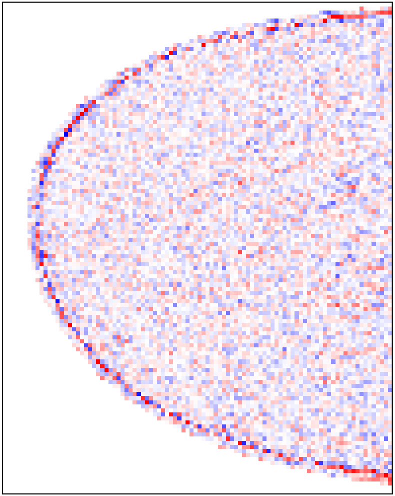

SNR 20dB

# Influence of Noise

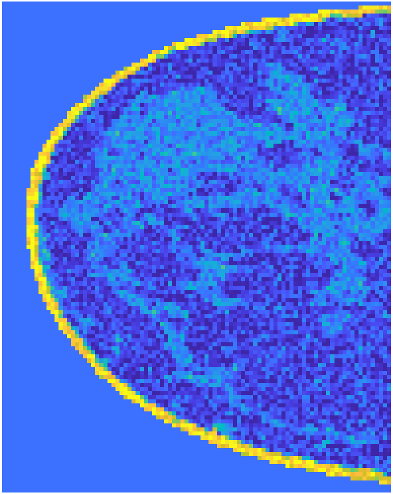

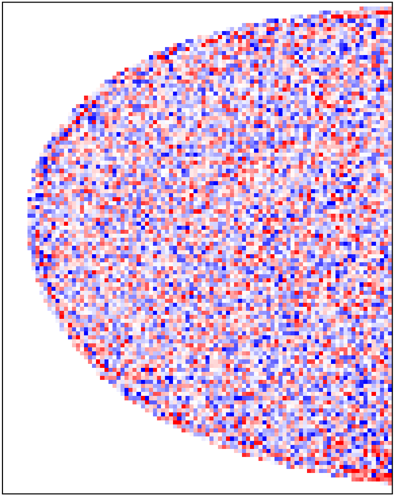

SNR 10dB

# Influence of Noise

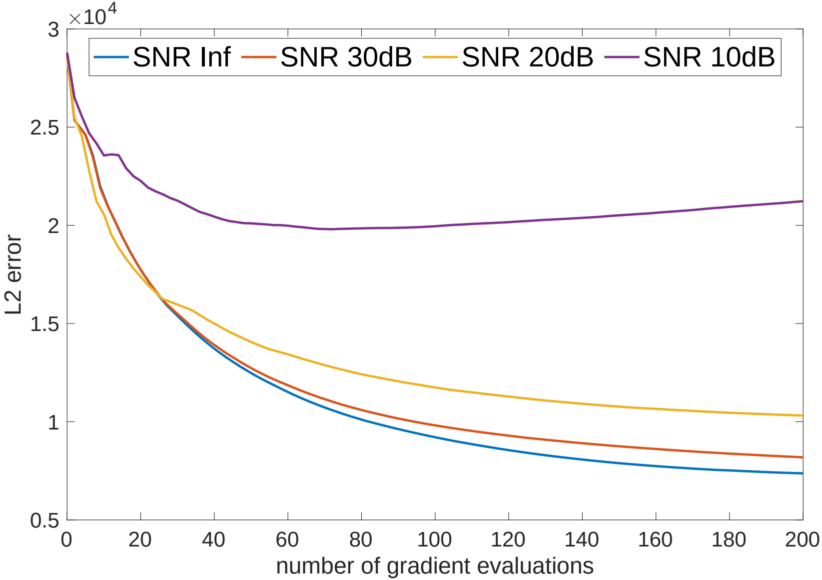

# Mathematical Modelling (simplified)

**Quantitative Photoacoustic Tomography (QPAT)**

radiative transfer equation (RTE) + acoustic wave equation

$$(v \cdot \nabla + \mu_a(x) + \mu_s(x))\, \phi(x, v) = q(x, v) + \mu_s(x) \int \Theta(v, v')\phi(x, v')dv',$$

$$p^{PA}(x, t = 0) = p_0 := \Gamma(x)\mu_a(x) \int \phi(x, v)dv, \qquad \partial_t p^{PA}(x, t = 0) = 0$$

$$(c(x)^{-2}\partial_t^2 - \Delta)p^{PA}(x, t) = 0, \qquad f^{PA} = Mp^{PA}$$

**Ultrasound Computed Tomography (USCT)**

$$(c(x)^{-2}\partial_t^2 - \Delta)p^{US}(x, t) = s(x, t), \qquad f^{US} = Mp^{US}$$

**Step-by-step inversion**

1. $f^{US} \to c$: acoustic parameter identification from boundary data.
2. $f^{PA} \to p_0$: acoustic initial value problem with boundary data.
3. $p_0 \to \mu_a$: optical parameter identification from internal data.